Photovoltaic Panel Cooling by Atmospheric Water Sorption-Evaporation Cycle

Renyuan Li[1], Yusuf Shi[1], Mengchun Wu[1], Seunghyun Hong[1], and Peng Wang[1, 2,*]

1. Water Desalination and Reuse Center, Division of Biological and Environmental Science and Engineering, King Abdullah University of Science and Technology, Thuwal 23955-6900, Saudi Arabia

2. Department of Civil and Environmental Engineering, The Hong Kong Polytechnic University, Hung Hom, Kowloon, Hong Kong, China

* Address correspondence to peng.wang@kaust.edu.sa; peng1.wang@polyu.edu.hk

Abstract

More than 600 gigawatts (GW) photovoltaic (PV) panels are currently installed worldwide, with the predicted total capacity increasing very rapidly every year. One essential issue in PV conversion is massive heat generation of PV panel under sunlight, which represents 75% to 96% of the total absorbed solar energy and thus greatly increases temperature and decreases the energy efficiency and lifetime of the PV panel. In this work, we demonstrate a new and versatile PV panel cooling strategy that employs sorption-based atmospheric water harvester (AWH) as effective cooling component. The AWH based PV cooling provides an averaged cooling power of 295 W/m^2 and lowers temperature of PV panel by at least 10 ^{o}C under 1.0 kW/m^2 solar irradiation in lab conditions. It delivers 13% to 19% increase in electricity generation of the commercial PV panels in outdoor field tests conducted in winter and summer in Saudi Arabia. The AWH based PV panel cooling strategy has little geographical constrain in its application and is promising in improving electricity productivity of existing and future PV plants, which can be directly translated into less CO_2 emission or less land occupation by PV setup. As solar power is taking a central stage in the global fight against climate change, AWH based cooling represents a solid force toward sustainability.

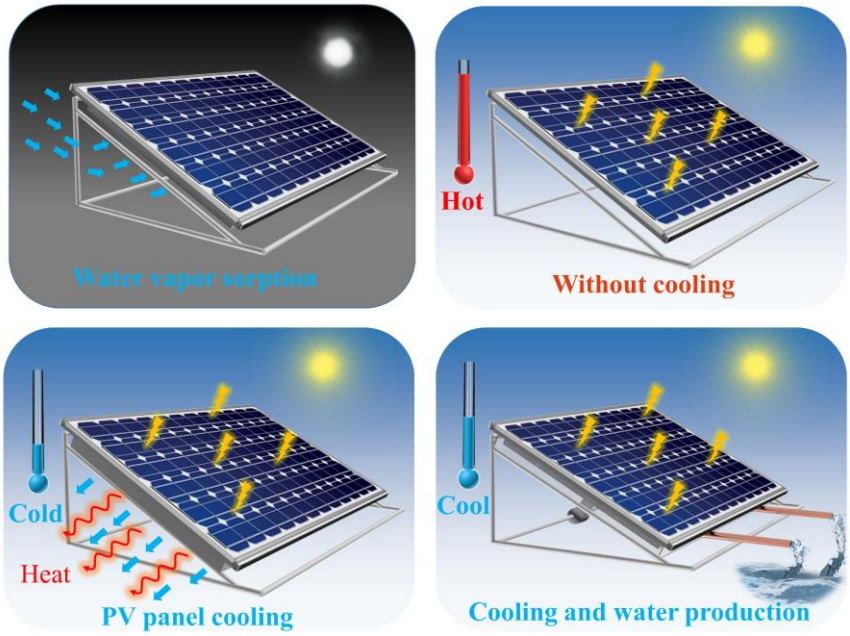

Solar energy is the most abundant, inexhaustible and clean renewable energy resource till date. A photovoltaic (PV) system converts solar energy into usable electricity and is currently the most popular means of solar energy utilization.[1,2] In 2019, the total installed capacity of solar PV panels worldwide reached 600 gigawatts (GW) and it is projected that the global PV capacity will reach 1500 GW by 2025 and 3000 GW by 2030.[3] Generally, only 6%–25% of the absorbed solar energy is converted to electricity by commercial solar PV panels, with the rest inevitably converted to heat with a heat power of around 600 to 900 W/m^2 under one-sun illumination.[4,5] The heat increases the temperature of the solar panel up to 40 ^{o}C above the ambient temperature.[6] The raised temperature of the PV panel is detrimental to the energy conversion of the panel, with a reported 0.4-0.5% energy efficiency loss for each degree of temperature rise.[7-9] In addition, high temperature degrades the lifetime of the solar panel.[10,11] Thus, effective and versatile cooling of the PV panel is highly important for effective and long-term power generation in existing as well as future solar power plants.

The current PV panel cooling technologies can be divided into two categories: active cooling and passive cooling.[12-14] Active cooling uses coolant such as water or air to dissipate heat from the surface of PV panel.[15-17] While it has high cooling efficiency, it requires complicated engineering design and needs energy to power up condenser and re-flux coolant.[18,19] For example, water spraying PV cooling system can effectively reduce the PV temperature. However, a large quantity of liquid water is required and subsequently wasted during cooling. Forced airflow circulation process can be used to cool down PV panel without the consumption of water, but a heatsink is required and turbulent airflow would make the heatsink highly unstable.[13] On the other hand, passive cooling relies on such natural processes as heat radiation and natural ventilation to enhance the heat dissipation.[20-25] While passive cooling has simple system design and small energy consumption, it provides relatively small cooling power.[26] For example, radiative cooling can provide a cooling power of 40-120 W/m^2 only under clear and cloudless weather. Thus, engineering simple, inexpensive, and effective design for solar panel cooling is highly sought after.

In this work, we demonstrate a simple but effective new PV cooling strategy to enhance the power output of commercial PV panels. The cooling component in the design is an atmospheric water harvester (AWH). The AWH harvests atmospheric water vapor by the sorption-based approach in the evening and at night, vaporizes and thus releases the sorbed water by utilizing the waste heat from the PV panel as energy source during daytime.[27-30] Due to the large enthalpy of water vaporization (~2450 J/g), the evaporation of the sorbed water takes away large amount of heat and thus keeps the PV panel in a relatively low temperature under solar irradiation.[31] The AWH in this work is directly attached on the backside of a commercial PV panel and extracts and stores large quantity of water from air even with very low relative humidity (RH) (i.e. <35%) in the evening and during night when the PV panel is not operating. During daytime, as the PV panel is heated up and its conducts heat to the AWH cooling layer. The heat in turn drives evaporation of the stored water in the AWH accordingly, leading to a lowered PV panel temperature. Our results show the AWH can provide an averaged cooling power of 295 W/m^2 when the solar cell is exposed under one Sun illumination, leading to >10 ^{o}C decrease in the temperature and up to 15% increase in electricity generation of the solar cell relative to the case in the absence of the AWH in lab conditions. The outdoor field tests conducted in summer and winter achieved an electricity generation enhancement of ~19% and ~13%, respectively, and also confirmed its performance stability. The advantages of this AWH based PV cooling approach are (1) it has a simple engineering design; (2) its application is globally suitable and not restricted by availability of liquid water; (3) the cooling process is solely waste-heat based and does not entail any additional energy consumption; (4) the design of the system allows for flexibility so that the evaporated water can be easily collected as fresh water for other foreseeable beneficial uses.

Results and discussion

In this work, a proof-of-concept of the atmospheric water sorption and evaporation based cooling strategy is provided by using a commercial PV panel combined with a hydrogel based AWH, consisting of CNT-embedded cross-linked polyacrylamide (PAM) as substrate and calcium chloride as water vapor sorbent (PAM-CNT-$CaCl_2$). The hygroscopic salt $CaCl_2$ in the PAM hydrogel makes the AWH able to capture a large quantity of water vapor from the air due to its extremely high water affinity. The PAM hydrogel framework endues the composite with a gel-like solid form, which holds $CaCl_2$ and its sorbed water at night and allows for controlled evaporation taking place during daytime.

Theoretical modeling (Supplementary note 1) was conducted first to qualitatively evaluate the mass and heat transfer within such a PV-cooling system, which guided the experimental design later on. The details and results of the modelling can be found in SI. Based on the heat transfer model, increasing emissivity of cooling material can further increase the cooling performance through thermal radiation. Thereby, CNT was present in the hydrogel matrix to increase the emissivity and to promote heat dissipation efficiency through thermal radiation of the AWH cooling layer (Supplementary Figure 1).[32]

Synthesis of PAM-CNT-$CaCl_2$ hydrogel cooling layer

The PAM-CNT-$CaCl_2$ hydrogel was fabricated following a similar procedure reported in literature, which is schematically presented in Figure 1.[29] The PAM-CNT hydrogel matrix was fabricated by in-situ polymerization of AM monomer in a CNT aqueous dispersion (step 1 of Figure 1). Freeze-drying was used to remove water solvent and to build a porous structure in the PAM-CNT hydrogel. The freeze-dried hydrogel was then infiltrated by a $CaCl_2$ aqueous solution to impregnate $CaCl_2$ into the hydrogel matrix (step 2 of Figure 1). The PAM hydrogel gives the composite a gel-like solid form even after a large amount of water is sorbed. Finally, the hydrogel was attached to the backside of the PV panel to serve as the cooling layer (step 3 of Figure 1).

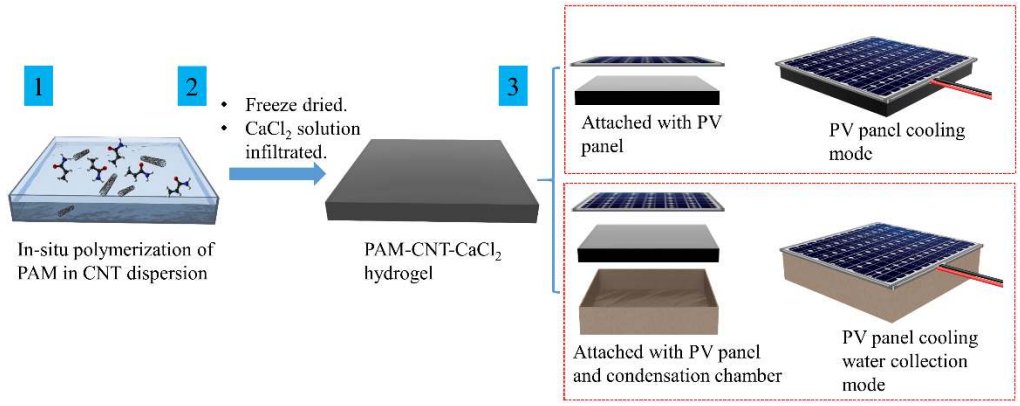

Figure 1. Schematic of PAM-CNT-$CaCl_2$ cooling layer synthesis process (step 1 and 2) and two PV panel working modes (step 3).

The SEM images of the freeze-dried PAM-CNT hydrogel (Figure 2a and b) clearly reveal the porous structure of the hydrogel. The average pore diameter is estimated to be around 3 μm and the wall thickness is ~100 nm. The size and thickness of the PAM-CNT-$CaCl_2$ hydrogel can be easily adjusted according to the shape and scale of PV panel by using a pre-fabricated mold or just by knife cutting. Figure 2 (c-e) shows the digital photos of a PAM-CNT-$CaCl_2$ hydrogel that was cut by a knife and attached on the backside of a commercialized PV panel, before, during, and after PV cooling test. The hydrogel can automatically and firmly attach to the backside of PV panel without additional assistance due to the rich hydrogen bonds of the hydrogel.

The water vapor sorption property of the PAM-CNT-$CaCl_2$ hydrogel under static RH mode was conducted on a simultaneous thermal analyzer (STA) coupled with module humidity generator (Figure 2 f-h). The sorption curves of static RH test present the weight change profiles of the sample during the tests, while the derivative weight change curves reflect the instant sorption rates during the test. As shown in Figure 2 (f), when RH was at a low level (i.e. 35%), the final water uptake value was ~50% compared with the original weight of the dehydrated PAM-CNT-$CaCl_2$ hydrogel. The sorption rate increased to its peak value (~1.5 mg/g min) within 1 hour, and then slowly dropped back to zero at the end of the test. A similar trend of the sorption rate could be found when the RH was set at 60 and 80%, respectively. The amount of absorbed water by PAM-CNT-$CaCl_2$ at RH 60% and 80% was ~99% and ~160% in 15 hours, respectively. However, the peak values of derivative weight change of the hydrogel at RH 60% and 80% are quite similar (i.e. 4.4 vs 4.6 mg/g min, Figure 2 g and h). The full data plot of STA test, including both sorption and desorption processes, can be found in Supplementary Figure 2.

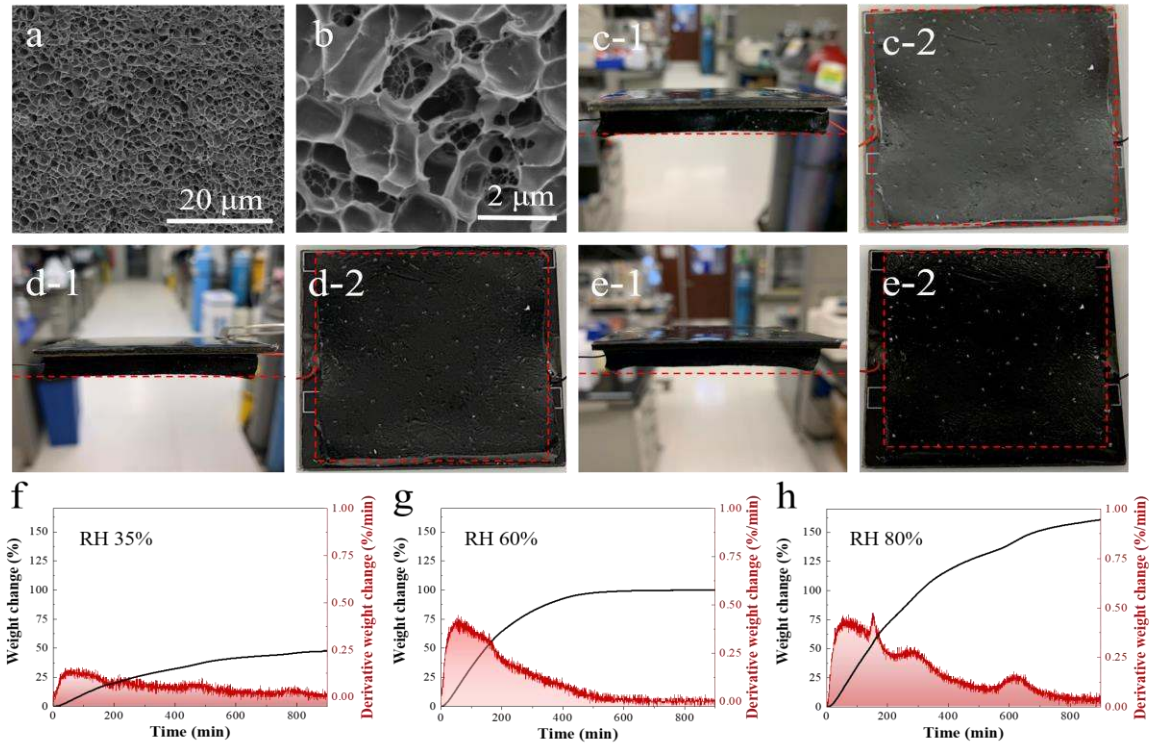

Figure 2. (a) SEM image and (b) magnified SEM image of freeze-dried PAM-CNT hydrogel. Digital photo of PAM-CNT-$CaCl_2$ hydrogel attached on the backside of a commercialized PV panel (c) before water vapor desorption; after water vapor desorption for (d) 1.5 h and (e) 3 h under simulated sunlight strength of 1 kW/m^2. The hydrogel was cut into a squared shape by knife. The dash lines indicate the thickness change of the hydrogel during test, and the dash square indicates the dimension change of the hydrogel during the test. (f)-(h) Water vapor sorption properties of PAM-CNT-$CaCl_2$ hydrogel under different RH conditions at 25 ºC.

PV panel cooling performance under simulated lab conditions

PV panel cooling experiments were performed under simulated sunlight first to investigate the effectiveness of the AWH cooling layer. Based on the I-V curves obtained, the characteristics (i.e. open circuit voltage (V_{oc}), filling factor (FF) efficiency, and maximum power output (P_{max})) of the PV panel were calculated and compared.

As can be seen in Figure 3 (a), the equilibrium temperature of the PV panel under 0.8 kW/m^2 sunlight irradiation was ~57 ºC (without cooling layer) and 45 ºC (with cooling layer). The temperature profiles of the PV panel under 1.0 W/m^2 and 1.2 W/m^2 sunlight irradiation are shown in Figure 3 (b), and (c), where a temperature drop of 10-15 ºC was achieved when the AWH cooling layer was employed. The weight loss profile (Figure 3 d) of the hydrogel shows the amount of the water evaporated during the test. As can be seen clearly, the water evaporation rate (the slope of the curves) was highly dependent on the irradiated light intensity. For the conditions of 0.8, 1.0, and 1.2 kW/m^2 light irradiation, around 2.75, 3.25, and 3.65 g of water was evaporated

throughout the period of test. The averaged cooling power (P) induced by water evaporation under each condition was calculated based on following equation.

$$P = \frac{\Delta H_{vap} \times \Delta m}{t \times A} \quad (1)$$

Where ΔH_{vap} is the enthalpy of vaporization of water (2450 J/g), Δm is the weight loss of hydrogel due to water evaporation, t is test time (3 hours), and A is surface area of hydrogel (25 cm^2). Thus, the cooling power of AWH cooling layer under 0.8, 1.0, and 1.2 kW/m^2 sunlight irradiation is 249.5, 294.9, and 331.2 W/m^2, respectively. These values are much higher than the radiative cooling (i.e. 40-120 W/m^2).[33]

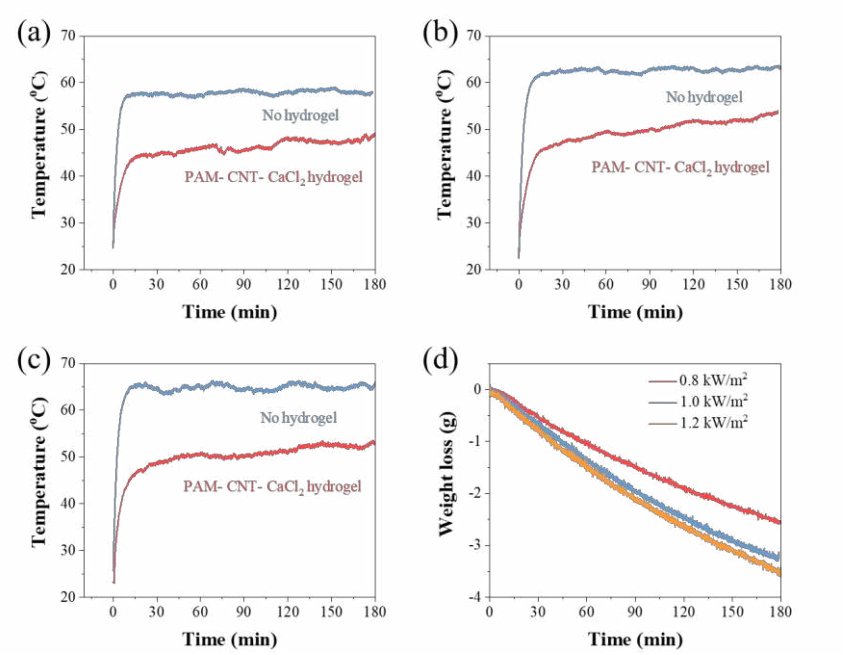

Figure 3. Temperature profile of the PV panel with/without AWH cooling layer under (a) 0.8 kW/m^2, (b) 1.0 kW/m^2, and (c) 1.2 kW/m^2, (d) weight loss profile of the hydrogel during the test. The original weight of hydrogel was 11.0 g.

The I-V curves of the PV panel with and without AWH cooling layer under 0.8 kW/m^2 sunlight irradiation are shown in Supplementary Figure 7 (a) and (b). In both occasions, the currents decreased with increasing voltages and the I-V curves corresponding to longer sunlight irradiation occurred below the curves corresponding to shorter irradiation time, indicating a poorer performance under longer irradiation. Similar I-V curves were observed when the light intensity was increased to 1.0 kW/m^2. Besides, the I-V curves in the presence of AWH cooling layer presented a delayed performance drop while the one without quickly reached its equilibrium of its minimized performance (Supplementary Figure 8 a and b).

In the equatorial or low latitude regions such as the Middle East and Africa, the peak sunlight intensity can be more than 1.2 kW/m^2 during the mid-day of summer.[34-36] Under 1.2 kW/m^2 solar irradiation, the current of PV panel quickly dropped to its minimal value within 15 minutes, indicating a quick performance drop under strong light condition. In the presence of the AWH

cooling layer, the IV curve shows a postponed performance drop (Supplementary Figure 9 a and b).

The characteristics of the PV panel (i.e. V_{oc}, FF, P_{max}, and efficiency) were recorded under varied test conditions (Figure 4). When the PV panel was operating without the AWH cooling layer, V_{oc} of the PV panel under 0.8, 1.0, and 1.2 kW/m^2 sunlight irradiation quickly dropped from 5.68 V to 5.25 V, 5.70 to 5.20 V, and 5.71 V to 5.18 V by the end of the first 15 minutes, followed by a plateau region thereafter. In contrast, when the AWH cooling layer was present, the V_{oc} of the PV panel dropped from 5.70 V to 5.45 V, 5.75 to 5.40 V, and 5.76 V to 5.41 V by the end of the first 15 minutes, followed by a slow drop to 5.33 V, 5.30, and 5.26 V after 3 hours test (Figure 4 a).

A similar trend was observed for FF, with the AWH cooling layer delivering a better FF than without (i.e. 71% vs. 69%, 70% vs. 68% for 0.8 and 1.0 kW/m^2 light irradiation, respectively). Under 1.2 kW/m^2 sunlight irradiation, the one with AWH cooling layer shows a higher FF value than that without until the end of 105 min. However, by the end of the 3 hours test, the FF values of both cases were similar (Figure 4 b).

In the absence of the AWH cooling layer, within the first 30 minutes, the efficiency of the PV panel quickly dropped from 14.8% to 13.5%, 13.7% to 11.8% and 14% to 11.9% for the conditions of 0.8, 1.0, and 1.2 kW/m^2 sunlight irradiation, respectively. In contrast, in the presence of the AWH cooling layer, the efficiency of the PV panel preserved the value of 14.0%, 12.6% and 12.75% by the end of the experiment. (Figure 4 c).

The maximum power output, which indicates the electrical power generation ability of the PV panel, is also compared. The P_{max} of PV panel without the cooling layer quickly dropped from 221 mW to 193 mW (0.8 kW/m^2), 255 mW to 225 mW (1.0 kW/m^2), and 315 mW to 270 mW (1.2 kW/m^2) within the first 15 minutes. The P_{max} of PV panel cooled by the AWH layer slowly dropped to 208 mW (0.8 kW/m^2) and 222 mW (1.0 kW/m^2) after 30 minutes sunlight irradiation and these values remained almost unchanged until the end of the 3 hours test. For the condition of 1.2 kW/m^2 sunlight irradiation, the P_{max} slowly dropped from 317 mW to 290 mW by the end of the first hour and further to 283 mW by the end of the test. Therefore, the AWH cooling layer is beneficial to promote the performance of PV panel under various sunlight strength (Figure 4 d).

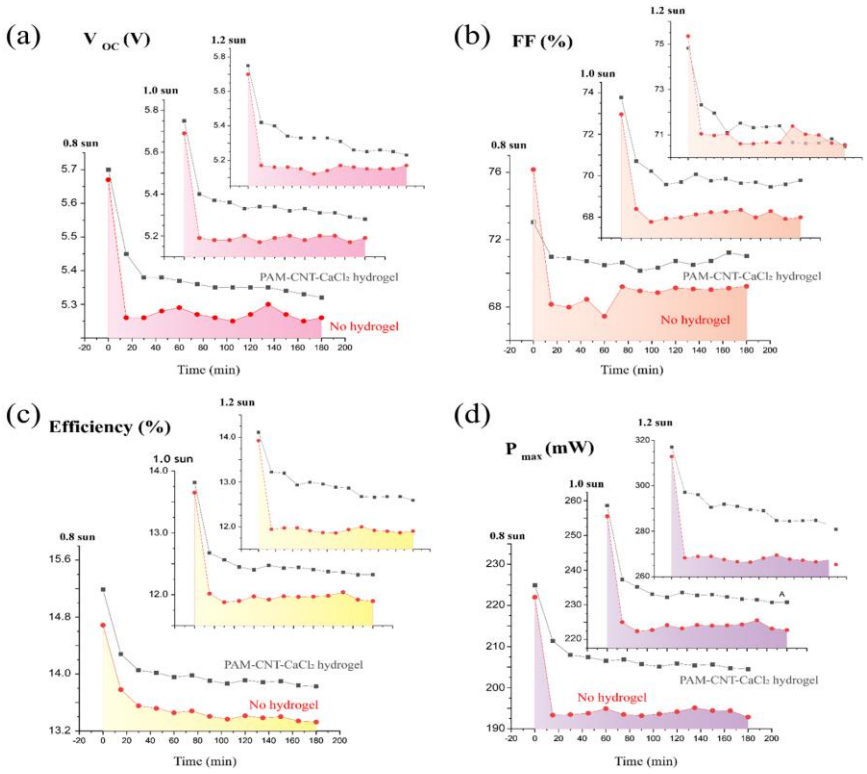

Figure 4. Parallel comparison of (a) V_{oc}, (b) FF, (c) efficiency, and (d) P_{max}, under light intensity of 0.8, 1.0, and 1.2 kW/m^2, respectively. The data points of t=90 min and t=180 min are also summarized in Supplementary Table 2.

With the AWH cooling layer, the averaged energy efficiency improvement of the PV panel is calculated to be 5.2, 5.0, and 7.3% under 0.8, 1.0 and 1.2 kW/m^2 condition, respectively and P_{max} is enhanced by 6.7, 5.3, and 7.4%, respectively. All these results clearly demonstrate that the temperature of the solar panel can be significantly decreased by evaporation of water from the AWH, which effectively diminishes the effect of the temperature increase and results in a better energy conversion performance.

When the light intensity was 1.2 kW/m^2, the enhanced PV performance was distinctly higher than those recorded under 0.8 and 1.0 kW/m^2, which is explained as follows. In this work, hygroscopic salt $CaCl_2$ is used to capture water vapor from the air and the cooling of the PV panel relies on the evaporation of water from $CaCl_2$ aqueous solution inside hydrogel. In other words, the $CaCl_2$ solution is being gradually concentrated in the course of the evaporation-induced cooling, which requires a gradually increasing temperature to drive further evaporation. Under a weak light condition, the evaporation rate of $CaCl_2$ solution is suppressed due to a low temperature of the PV panel. Under a strong light condition (i.e. 1.0-1.2 kW/m^2), due to the higher temperature of the PV panel, the evaporation rate is enhanced.

It is worth pointing out that, after most of the water in the AWH is released, the evaporation rate is slowed down and the heat dissipation process is suppressed accordingly. Thus, towards the end of the test, the temperature difference between the presence and absence of the AWH cooling layer

is reduced (Supplementary Figure 9 (c)-(f)). It is expected, when a larger quantity of AWH is applied, the effect of the AWH assisted cooling will be more pronounced for longer period.

A simulated full-day experiment was conducted. Figure 5 (a) compares the actual sunlight strength in real condition (red color, data obtained from NOAA)[39] and the applied sunlight in the test, showing a high level of similarity. Figure 5 (b) shows the V_{oc} change of the PV panel with and without the AWH cooling layer during the test. For the V_{oc} change curves obtained before the simulated time of 15:00 (i.e., 8 hours test), the absolute value of voltage decreased, which was resulted from the increased temperature of PV panel. For the curves after the simulated time of 15:00, an increment of V_{oc} was observed. This is because the light was adjusted to a lower strength, which lowered the PV panel's temperature. The averaged V_{oc} value of the PV panel with the AWH cooling layer showed 0.2 V higher than that without cooling layer. The P_{max} with the AWH cooling layer was constantly higher value than that without (Figure 5c). Due to the fact that the heat generated from the PV panel is not significant under weakened sunlight (i.e. 400, 600 W/m^2), the differences in temperature and P_{max} values between the PV panel with and without the cooling layer were not considerable.

When the light intensity is strengthened (i.e. 800-1060 W/m^2), the AWH is heated up, the evaporation process is enhanced, the heat is compensated through evaporation process, and the temperature of the PV panel is reduced. In the absence of the AWH, the increased PV panel temperature led to a quiet distinct P_{max} value under strong sunlight irradiation (3-9 h in the test) than the one in the presence of the AWH. Based on P_{max}, an overall 15.2% increase in power output of the PV panel was obtained with the AWH cooling layer, indicating its capability of consistently cooling down PV panel for elongated period.

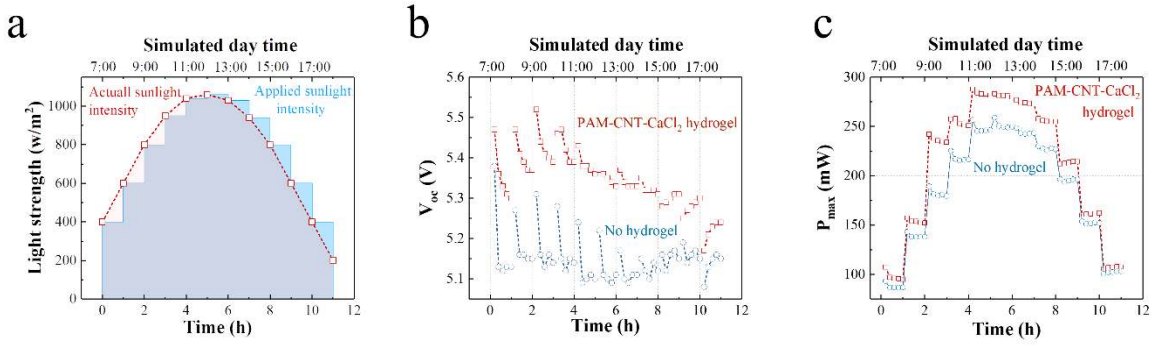

Figure 5. (a) Actual sunlight strength during a day (data obtained from NOAA) and simulated sunlight strength during the experiment. (b) V_{oc} and (c) P_{max} of PV panel with/without hydrogel cooling layer under simulated daylight.

PV panel cooling performance under real outdoor conditions

To demonstrate the performance versatility and stability of the AWH-based PV panel cooling system, two complete sorption-evaporation outdoor tests in two seasons (summer and winter of Saudi Arabia) and a 7-day outdoor stability test were performed. All three outdoor tests were conducted inside KAUST campus, Saudi Arabia (GMT+3，22°19'06.1"N 39°06'15.0"E). The details of the outdoor tests, including experimental setup (photos), solar irradiance, weather

conditions, hydrogel weight change, temperature and power of PV panel, etc. were monitored real-time and can be found in Supplementary note 2. The performance improvement was calculated by following equation:

$$E = \left(\frac{\eta_{with\ hydrogel}}{\eta_{without\ hydrogel}} - 1\right) \times 100\% \quad (2)$$

Where E denotes the efficiency enhancement, $\eta_{\text{with hydrogel}}$ and $\eta_{\text{without hydrogel}}$ are electricity conversion efficiency of PV panel with and without hydrogel cooling layer attached, respectively. The first test was conducted on August 14 and 15, 2019 (summer), during which the comparison of the same PV with and without AWH cooling layer was conducted. Considering the daily difference in solar irradiance, an efficiency enhancement of ~19.0% was obtained. This value is slightly higher than the one observed in the lab condition (i.e., 15.2%), presumably due to outdoor wind-field-facilitated evaporation and heat dissipation in the field conditions. The second outdoor test was conducted from November 30 to December 5, 2019 (winter) with a similar experimental setup (Supplementary note 2). A 13.5% efficiency enhancement was achieved with the AWH cooling layer in comparison to the one without. This is a considerable improvement given that the PV worked in a lower ambient temperature than in the first summer field test. The above two outdoor test conducted in different seasons both produced satisfactory performances and thus successfully demonstrate the feasibility and versatility of the concept of utilizing atmospheric water as coolant to cool down the PV panel.

In addition, a 7-cycle outdoor field test was performed to confirm the stability and recyclability of such a system, including the water sorption and desorption capacities of the hydrogel, its contact with PV panel, its cooling performances, along with the resultant electricity generation performance by PV. The test was performed between December 27, 2019 at 00:00 and January 2, 2020 and the results successfully demonstrate both structural and performance stability of the cooling layer design (Supplementary note 2).

Based on the outdoor test results as well as the model results, further performance improvement of AWH-based PV cooling can start with AWH with enhanced vapor sorption capacitiy and kinetics. To this end, hosting sorbents within macroporous substrates deserves research attention. Based on the heat transfer model, increasing emissivity of cooling material can further increase the cooling performance through thermal radiation. In the meanwhile, proper increase of thermal conductivity of the cooling layer will further enhance the overall cooling performance.

PV panel cooling and atmospheric water collection

The AWH based PV panel cooling can be modified to produce clean water by integrating the hydrogel cooling layer within a water condensation chamber with enlarged heat dissipation surface area (Figure 6 a). In one experiment, an aluminum condensation chamber was attached right beneath the AWH cooling layer (dimension $5 \times 5 \times 0.5$ cm^3), which led the surface temperature of the panel stable at ~50 ^{o}C during the test (Figure 6b). As can be seen in Figure 6 (c), the efficiency of PV panel in the presence of the condensation chamber decreased from 14.6% to 13.25% at the first 15 min, and finally was stabilized at 13%, which was higher than the efficiency of the original PV panel at steady state (12.5%). Meanwhile, the P_{max} of PV panel with the condensation chamber

decreased from 267 mW to 246 mW by the end of the experiment, which was higher than the steady P_{max} of original PV panel (236 mW, Figure 6d). At the end of the experiment, around 2.0 g of water was collected and the calcium concentration in the collected water was below the detection limit of the instrument (i.e. 0.5 ppb). It has to be mentioned that the PV panel used in this experiment was different from the one in the previous section and thus a direct performance comparison was not made. The results demonstrate that the AWH-based PV panel cooling system can be extended to produce liquid water.

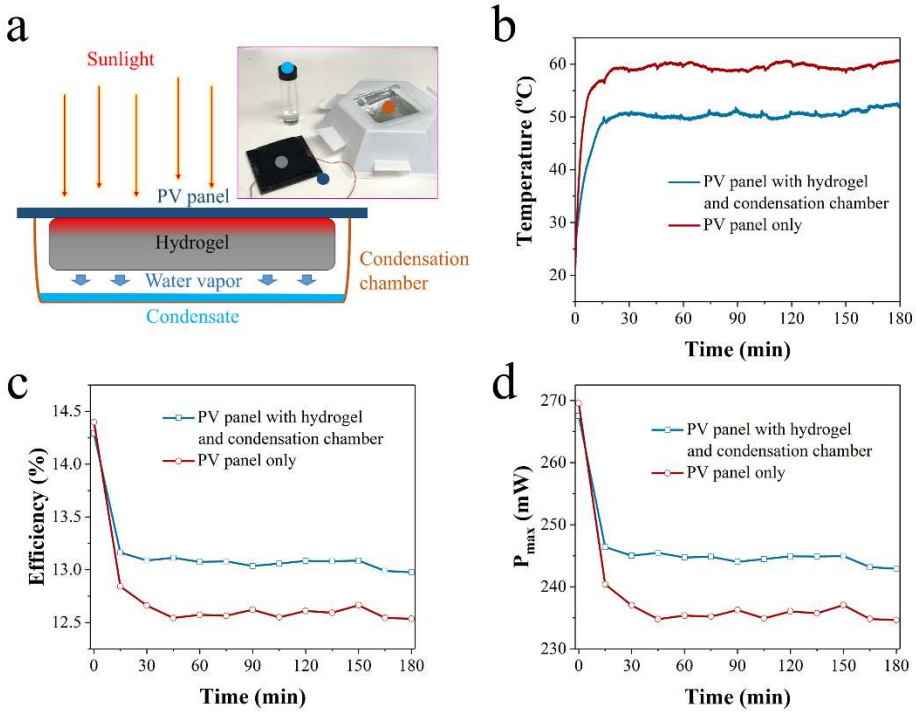

Figure 6. (a) Schematic and digital photo of test setup for PV panel cooling and water collection. The components with the colored dots in the digital photo indicate the corresponding sections in the scheme with the same color. (b) The temperature profile of the PV panel top surface. Comparison of efficiency (c) and P_{max} (d).

In arid and semi-arid regions that have frequent dust storms or dusty conditions, the surface of PV panel is typically and constantly covered with a layer of dust which blocks solar irradiation. It has been reported that a single dust storm can reduce the power output of PV panel by 20% and more than 50% of power output reduction may be resulted in if PV panel fails to be properly cleaned over six months.[37] Water spray is one of the most commonly used methods for PV panel cleaning and this work provides a solution of harvesting atmospheric water and thus cleaning PV panel in dry regions where getting liquid form water is challenging. Furthermore, fresh water supply in the arid and semi-arid regions largely relies on uneconomical and inefficient long-distance water transportation.[38-40] This work provides an attractive solution for solar farms to cool down PV panels and simultaneously produce clean water for dust cleaning for PV panel and/or potable purpose.

Conclusion

In conclusion, this work successfully applies atmospheric water sorption-desorption cycle to cool down PV panel. A cooling power of 295 W/m^2 under 1000 W/m^2 solar irradiation was achieved and thus reduces temperature of PV panel by at least 10 ^oC during operation under lab conditions. The outdoor field tests in summer and winter at Saudi Arabia show that the AWH cooling leads to a ~19% and ~13% increase in the electricity generation by commercial PV respectively. As the global PV installation capacity is predicted to reach 1500 GW by 2025, there would be >150 GW more electricity to be produced should all PV panels be cooled by this approach by then. This amount of additional electricity can be directly translated into $>8.52\times10^7$ metric tons less of coal per year, $>1.48\times10^8$ tons of CO_2 emission reduction per year, or 750 km^2 (~186,000 acres) of land to be freed from PV occupation, assuming 20% of solar PV electricity generation efficiency. Further improvement of AWH-assisted PV cooling should include enhancing water vapor sorption/desorption kinetics and thus capacity by the AWH, material corrosion, etc. The AWH assisted PV cooling is widely applicable to all kinds of PV installation at any scale, from a single household to large industrial PV farm, and thus is a meaningful contribution to the ongoing effort to fight climate change.

Methods

Chemical and Materials

Acrylamide monomer (AM, 99%), N,N'-methylenebis(acrylamide) (MBAA, 99%), N,N,N'N'-Tetramethylethylenediamine (TEMED, 99%), carbon nanotube (CNT, multi-walled), nitric acid, and calcium chloride ($CaCl_2$, 99%) were purchased from Sigma-Aldrich. Potassium persulfate (KPS, 99%) was purchased from Acros Organics. All chemicals were used without further purification. Deionized (DI) water (18.2 MΩ, from Milli-Q system) was used throughout the experiments. Commercial photovoltaic (PV) panel was purchased from SUNTHING GOOD Co., Ltd.

Lab conditions:

Both the room temperature and relative humidity (RH) were controlled by heating, ventilation, and air conditioning (HVAC) system. The room temperature was maintained at 22 ^{o}C, and the RH was maintained at 60% (absolute humidity: 11.6 grams of water per cubic meter of air (g/m^3)).

Fabrication of Polyacrylamide (PAM)-CNT-$CaCl_2$ Hydrogel

Pretreatment of CNT. The pretreatment of CNT was followed with a previous work.[30] Briefly, 6.0 g of as-purchased CNT was dispersed in a mixture of sulfuric acid (97%, 180 mL) and nitric acid (70%, 60 mL). After refluxed for 4 h at 70 ^{o}C, the dispersion was sonicated for 2 hours, filtrated and washed by DI water thoroughly before use.

Preparation of PAM-CNT-$CaCl_2$ hydrogel. 25.0 g of AM was dissolved in 125 mL of 0.5 mg/mL CNT aqueous dispersion, followed by purging with nitrogen to eliminate dissolved oxygen. Then, 0.125 g of KPS and 0.048 g of MBAA were added into the dispersion as initiator and cross-linking agent, respectively. Finally, 2 mL of TEMED was added as cross-linking accelerator. After settling the mixture overnight under a nitrogen atmosphere, the PAM-CNT hydrogel was obtained. To load $CaCl_2$ into the hydrogel, the as-prepared PAM-CNT hydrogel was first freeze-dried at −80 ^{o}C (FreeZone 2.5 plus, LABCONCO), followed by immersing the dry hydrogel in 125 mL $CaCl_2$ solution (0.4 g/mL) for 48 hours under ambient condition to fabricate the PAM-CNT-$CaCl_2$ hydrogel.

Material Characterization

Scanning electron microscopy image was obtained by a Zeiss Merlin field emission scanning electron microscope (FE-SEM). The metal content in the condensed water was examined by inductively coupled plasma-optical emission spectroscopy (ICP-OES, Agilent 5100) equipped with charge-coupled device (CCD detector) and charge injection device (CID detector).

Water vapor sorption and desorption tests were conducted on a simultaneous thermal analyzer (STA, Jupiter STA-449, NETZSCH) coupled with a modular humidity generator (MHG, ProUmid). The humidity generator was programmed to output nitrogen flow (100 mL/min) with predefined relative humidity (RH) and equilibration time. In more details, the STA furnace was programmed to simulate the temperature during the night (25 ^{o}C, water vapor sorption process). The flow temperature and flow rate of nitrogen carrier were set to be 25^{o}C, 100 mL/min while the

pre-designated RH was set to be 35, 60, and 80%, respectively. The selection of humidity parameter was based on the averaged global humidity distribution map. The relative humidity of 35, 60, and 80% represents most of the low (i.e., Central Australia, North Africa, Middle east, etc.), medium (i.e., Southern Africa, Northern Asia, Central Europe, North America, etc.), and high (i.e., South America, South Asia, Northern Europe, etc.) humidity regions around the world. Absolute humidity of STA in the water vapor sorption tests (25 ^{o}C, RH 35, 60, and 80%) was 8.1, 13.8, and 18.4 g/m^3, respectively. The STA furnace was first heated up to 85 ^{o}C to release the sorbed water and then cooled down to 25 ^{o}C for the water vapor sorption test.

Device assembly

The as-obtained PAM-CNT-$CaCl_2$ hydrogel was directly attached to the backside of commercialized PV panel due to its self-adhesion property. For PV panel cooling, the hydrogel attached PV panel was directly mounted on a homemade polystyrene frame, and the water evaporated from the hydrogel was directly released to the ambient air. For PV panel cooling with water collection, an additional condensation chamber was attached to cover the hydrogel and to collect the released water.

PV panel cooling test

The performance of the PV panel under different working conditions was tested on a Keithley-2400 source meter. The hydrogel-attached PV panel was first placed in the ambient with RH of 60% and temperature of 22 ^{o}C for 17 hours. Then the PV panel was directly exposed to the simulated sunlight (Oriel 94023A solar simulator, AM 1.5 filter). The mass change of the PV panel with the hydrogel was measured and recorded by an electronic balance connected to a computer. An IR camera (FLIR 655sc) was used to monitor and record the temperature change of the PV panel.

The simulated daylight was used to test the performance of the hydrogel-based cooling layer. The light intensity of solar simulator was tuned to reflect the daily variation of light strength during a day. The PV panel used in this work was composed of 9 pieces of solar cell in series combination. The effective area of the PV panel was 18.2 cm^2. Based on the mass transfer model (Supplementary note 1), the time required for the water vapor sorption process is highly dependent on the thickness of hydrogel. To ensure an effective sorption within a reasonable time frame, the attached hydrogel cooling layer was designed to be $5 \times 5 \times 0.5$ cm^3 in dimension and was exposed to the ambient condition (RH 60%, 22 ^{o}C) for 17 hours prior to the test. The experiments were performed under simulated sunlight with different light intensities (0.8, 1.0, and 1.2 kW/m^2) for 3 hours.

A simulated full-day experiment was conducted; the experiment was performed for 11 hours, starting from the simulated daytime of 7:00 am to 18:00 pm. The solar simulator was carefully adjusted every hour to reflect the daily light intensity variation while the data points were collected every 15 minutes. Three pieces of hydrogel with a dimension of $5 \times 5 \times 0.6$ cm^3 were stacked and attached to the PV panel. The detailed parameters can be found in Supplementary Table 3. [36]

The simulated solar intensity for the PV panel cooling and water collection mode was 1.0 kW/m^2. Dry weight of the hydrogel before water vapor sorption (i.e. weight of polyacrylamide and $CaCl_2$

along with its non-removable crystallized water) was 7.9 g, and the dimension of the hydrogel before water vapor sorption was ~4.2×4.2×0.3 cm^3. Water vapor sorption process was conducted by placing the dried hydrogel in lab condition for 17 hours. After the water vapor sorption process, the dimension of the hydrogel changed to ~5×5×0.5 cm^3, and the weight of the hydrogel was 14.1 g.

Acknowledgment

This work was supported by the King Abdullah University of Science and Technology (KAUST) Center Competitive Fund (CCF) awarded to the Water Desalination and Reuse Center (WDRC).

Author contributions

Peng Wang supervised the project; Renyuan Li, Yusuf Shi and Peng Wang conceived the idea and designed the experiments; Renyuan Li and Mengchun Wu performed the materials synthesis, characterization and performance investigation; Seunghyun Hong performed the graphic work; and Renyuan Li and Peng Wang co-wrote the pater. All authors discussed and commented on the manuscript.

Corresponding Author

Correspondence to Peng Wang

Data availability

The data that support the findings of this study are available from the corresponding author on reasonable request.

Competing interests

Peng Wang, Renyuan Li and Yusuf Shi have a patent application related to the work presented in this pater.

References

1 Parida, B., Iniyan, S. & Goic, R. A review of solar photovoltaic technologies. *Renew. Sust. Energ. Rev.* **15**, 1625-1636 (2011).

2 Yoshikawa, K. *et al.* Silicon heterojunction solar cell with interdigitated back contacts for a photoconversion efficiency over 26%. *Nat. Energy* **2**, 17032 (2017).

3 Jäger-Waldau, A. PV Status Report 2019. *Publications Office of the European Union, Luxembour* (2019).

4 Yang, D. & Yin, H. Energy Conversion Efficiency of a Novel Hybrid Solar System for Photovoltaic, Thermoelectric, and Heat Utilization. *IEEE T. Energy Conver.* **26**, 662-670 (2011).

5 van Helden, W. G. J., van Zolingen, R. J. C. & Zondag, H. A. PV thermal systems: PV panels supplying renewable electricity and heat. *Progress in Photovoltaics: Research and Applications* **12**, 415-426 (2004).

6 Makki, A., Omer, S. & Sabir, H. Advancements in hybrid photovoltaic systems for enhanced solar cells performance. *Renew. Sust. Energ. Rev.* **41**, 658-684 (2015).

7 Natarajan, S. K., Mallick, T. K., Katz, M. & Weingaertner, S. Numerical investigations of solar cell temperature for photovoltaic concentrator system with and without passive cooling arrangements. *Int. J. Therm. Sci.* **50**, 2514-2521 (2011).

8 Menke, S. M., Ran, N. A., Bazan, G. C. & Friend, R. H. Understanding Energy Loss in Organic Solar Cells: Toward a New Efficiency Regime. *Joule* **2**, 25-35 (2018).

9 Skoplaki, E. & Palyvos, J. A. On the temperature dependence of photovoltaic module electrical performance: A review of efficiency/power correlations. *Sol. Energy* **83**, 614-624 (2009).

10 Bredemeier, D., Walter, D., Herlufsen, S. & Schmidt, J. Lifetime degradation and regeneration in multicrystalline silicon under illumination at elevated temperature. *AIP Adv.* **6**, 035119 (2016).

11 Jordan, D. C. & Kurtz, S. R. Photovoltaic Degradation Rates—an Analytical Review. *Progress in Photovoltaics: Research and Applications* **21**, 12-29 (2013).

12 Bahaidarah, H. M. S., Baloch, A. A. B. & Gandhidasan, P. Uniform cooling of photovoltaic panels: A review. *Renewable and Sustainable Energy Reviews* **57**, 1520-1544 (2016).

13 Siecker, J., Kusakana, K. & Numbi, B. P. A review of solar photovoltaic systems cooling technologies. *Renew. Sust. Energ. Rev.* **79**, 192-203 (2017).

14 Shukla, A., Kant, K., Sharma, A. & Biwole, P. H. Cooling methodologies of photovoltaic module for enhancing electrical efficiency: A review. *Sol. Energ. Mat. Sol. C.* **160**, 275-286 (2017).

15 Teo, H. G., Lee, P. S. & Hawlader, M. N. A. An active cooling system for photovoltaic modules. *Appl. Energ.* **90**, 309-315 (2012).

16 Nižetić, S., Čoko, D., Yadav, A. & Grubišić-Čabo, F. Water spray cooling technique applied on a photovoltaic panel: The performance response. *Energ. Convers. Manage.* **108**, 287-296 (2016).

17 Odeh, S. & Behnia, M. Improving Photovoltaic Module Efficiency Using Water Cooling. *Heat Transfer Eng.* **30**, 499-505 (2009).

18 Nižetić, S., Giama, E. & Papadopoulos, A. M. Comprehensive analysis and general economic-environmental evaluation of cooling techniques for photovoltaic panels, Part II: Active cooling techniques. *Energ. Convers. Manage.* **155**, 301-323 (2018).

19 Bahaidarah, H., Subhan, A., Gandhidasan, P. & Rehman, S. Performance evaluation of a PV (photovoltaic) module by back surface water cooling for hot climatic conditions. *Energy* **59**, 445-453 (2013).
20 Stropnik, R. & Stritih, U. Increasing the efficiency of PV panel with the use of PCM. *Renew. Energ.* **97**, 671-679 (2016).
21 Chandel, S. S. & Agarwal, T. Review of cooling techniques using phase change materials for enhancing efficiency of photovoltaic power systems. *Renew. Sust. Energ. Rev.* **73**, 1342-1351 (2017).
22 Raman, A. P., Anoma, M. A., Zhu, L., Rephaeli, E. & Fan, S. Passive radiative cooling below ambient air temperature under direct sunlight. *Nature* **515**, 540, doi:10.1038/nature13883 (2014).
23 Zhu, L., Raman, A., Wang, K. X., Anoma, M. A. & Fan, S. Radiative cooling of solar cells. *Optica* **1**, 32-38 (2014).
24 Popovici, C. G., Hudişteanu, S. V., Mateescu, T. D. & Cherecheş, N.-C. Efficiency Improvement of Photovoltaic Panels by Using Air Cooled Heat Sinks. *Energy Procedia* **85**, 425-432 (2016).
25 Cuce, E., Bali, T. & Sekucoglu, S. A. Effects of passive cooling on performance of silicon photovoltaic cells. *Int. J. Low-Carbon Tec.* **6**, 299-308 (2011).
26 Nižetić, S., Papadopoulos, A. M. & Giama, E. Comprehensive analysis and general economic-environmental evaluation of cooling techniques for photovoltaic panels, Part I: Passive cooling techniques. *Energ. Convers. Manage.* **149**, 334-354 (2017).
27 Kim, H. *et al.* Water harvesting from air with metal-organic frameworks powered by natural sunlight. *Science* **356**, 430-434 (2017).
28 Kim, H. *et al.* Adsorption-based atmospheric water harvesting device for arid climates. *Nat. Commun.* **9**, 1191 (2018).
29 Li, R. *et al.* Hybrid Hydrogel with High Water Vapor Harvesting Capacity for Deployable Solar-Driven Atmospheric Water Generator. *Environ. Sci. Technol.* **52**, 11367-11377 (2018).
30 Li, R., Shi, Y., Shi, L., Alsaedi, M. & Wang, P. Harvesting Water from Air: Using Anhydrous Salt with Sunlight. *Environ. Sci. Technol.* **52**, 5398-5406 (2018).
31 Chan, H.-Y., Riffat, S. B. & Zhu, J. Review of passive solar heating and cooling technologies. *Renew. Sust. Energ. Rev.* **14**, 781-789 (2010).
32 Mizuno, K. *et al.* A black body absorber from vertically aligned single-walled carbon nanotubes. *P. Natl. Acad. Sci. U. S. A.*, pnas.0900155106 (2009).
33 Zeyghami, M., Goswami, D. Y. & Stefanakos, E. A review of clear sky radiative cooling developments and applications in renewable power systems and passive building cooling. *Sol. Energ. Mat. Sol. C.* **178**, 115-128 (2018).
34 Kandilli, C. & Ulgen, K. Solar Illumination and Estimating Daylight Availability of Global Solar Irradiance. *Energ. Sources. Part A.* **30**, 1127-1140 (2008).
35 Zell, E. *et al.* Assessment of solar radiation resources in Saudi Arabia. *Sol. Energy* **119**, 422-438 (2015).
36 http://www.cpc.ncep.noaa.gov/products/stratosphere/. *National Oceanic and Atmospheric Administration (NOAA).*
37 Adinoyi, M. J. & Said, S. A. M. Effect of dust accumulation on the power outputs of solar photovoltaic modules. *Renew. Energ.* **60**, 633-636 (2013).

523 38 Mekonnen, M. M. & Hoekstra, A. Y. Four billion people facing severe water scarcity. *Sci.*
524 *Adv.* **2**, e1500323 (2016).
525 39 Montgomery, M. A. & Elimelech, M. Water And Sanitation in Developing Countries:
526 Including Health in the Equation. *Environ. Sci. Technol.* **41**, 17-24 (2007).
527 40 Schiermeier, Q. Water risk as world warms. *Nature* **505**, 10–11 (2014).